

Optimizing cone-beam computed tomography exposure for an effective radiation dose and image quality balance

Ananda Amaral Santos^{1,2}, Brunno Santos de Freitas Silva^{2,3,*}, Fernanda Ferreira Nunes Correia², Eleazar Mezaiko², Camila Ferro de Souza Roriz¹, Maria Alves Garcia Silva^{1,2}, Deborah Queiroz Freitas⁴, Fernanda Paula Yamamoto-Silva^{2,3}

¹Department of Oral Radiology, University of Anápolis, Anápolis, GO, Brazil

²Department of Stomatologic Sciences, School of Dentistry, Federal University of Goiás, Goiânia, GO, Brazil

³Science Program in Dentistry, University of Anápolis, Anápolis, GO, Brazil

⁴Division of Oral Radiology, Department of Oral Diagnosis, Piracicaba Dental School, University of Campinas, São Paulo, Brazil

ABSTRACT

Purpose: The aim of this study was to evaluate the influence of different cone-beam computed tomography (CBCT) acquisition protocols on reducing the effective radiation dose while maintaining image quality.

Materials and Methods: The effective dose emitted by a CBCT device was calculated using thermoluminescent dosimeters placed in a Rando Alderson phantom. Image quality was assessed by 3 experienced evaluators. The relationship between image quality and confidence was evaluated using the Fisher exact test, and the agreement among raters was assessed using the kappa test. Multiple linear regression analysis was performed to investigate whether the technical parameters could predict the effective dose. *P*-values < 0.05 were considered to indicate statistical significance.

Results: The optimized protocol (3 mA, 99 kVp, and 450 projection images) demonstrated good image quality and a lower effective dose for radiation-sensitive organs. Image quality and confidence had consistent values for all structures (*P* < 0.05). Multiple linear regression analysis resulted in a statistically significant model. The milliamperage (*b* = 0.504; *t* = 3.406; *P* = 0.027), kilovoltage peak (*b* = 0.589; *t* = 3.979; *P* = 0.016) and number of projection images (*b* = 0.557; *t* = 3.762; *P* = 0.020) were predictors of the effective dose.

Conclusion: Optimized CBCT acquisition protocols can significantly reduce the effective radiation dose while maintaining acceptable image quality by adjusting the milliamperage and projection images. (*Imaging Sci Dent* 2024; 54: 159-69)

KEY WORDS: Cone-Beam Computed Tomography; Radiation Exposure; Radiation Dosimeters

Introduction

Despite the broad range of applications of cone-beam computed tomography (CBCT), this imaging modality carries a risk of stochastic effects due to its association with ionizing radiation, which results in a higher radiation dose compared

to 2-dimensional (2D) imaging. The effects of CBCT on human patients, including the threshold for harmful effects, remain uncertain.¹ Thus, there is a consensus that CBCT should only be prescribed when there are clear indications of its superiority over lower-dose radiographic exams.¹

A better-quality image is achieved when the technical parameters of the unit are set to a high-resolution mode, which is often correlated with higher dose values.² However, this could unnecessarily expose patients to higher radiation, posing a potential risk of cancer, particularly in children, who are more vulnerable to radiation.³ Therefore, according to Jaju and Jaju (2015),² the rational use of CBCT should involve obtaining acceptable quality images for diagnostic

This study was supported by grants from the National Council for Scientific and Technological Development (CNPq, grant 423885/2018-9 to F.P.Y.S.) and FUNADESP (4-1383/2022).

Received November 21, 2023; Revised January 11, 2024; Accepted January 11, 2024
Published online April 2, 2024

*Correspondence to : Prof. Brunno Santos de Freitas Silva
Department of Stomatologic Sciences, School of Dentistry, Federal University of Goiás,
Praça Universitária s/n, Setor Universitário - CEP 74605-220, Goiânia, GO, Brazil
Tel) 55-62-3434-4394, E-mail) brunno_santos@ufg.br

Copyright © 2024 by Korean Academy of Oral and Maxillofacial Radiology

This is an Open Access article distributed under the terms of the Creative Commons Attribution Non-Commercial License (<http://creativecommons.org/licenses/by-nc/3.0>) which permits unrestricted non-commercial use, distribution, and reproduction in any medium, provided the original work is properly cited.

Imaging Science in Dentistry · pISSN 2233-7822 eISSN 2233-7830

purposes with the lowest possible dose, referred to as “as low as diagnostically acceptable [ALADA]” in their paper.

Several CBCT exposure parameters directly influence the effective dose, such as exposure time, field of view (FOV) diameter, FOV height, kilovoltage, milliamperage, voxel size, and spatial resolution.⁴ Depending on the indication for CBCT, appropriate technical parameters should be selected to obtain a diagnostically acceptable and interpretable image.² However, optimizing the relationship between radiation dose and image quality is not a simple task, given the variety of parameters involved in the acquisition of CBCT images.⁴

Many studies have evaluated the radiation dose of CBCT under different parameters, but there is still a scarcity of studies investigating the optimization of different technical parameters to balance high image quality with lower doses.⁴ Thus, there is a need for further investigation of the dosimetric parameters of CBCT and their impact on image quality. Therefore, the aim of this study was to evaluate the influence of different CBCT acquisition protocols, with varying milliamperage, kilovoltage peak, and number of projection images, on the reduction of the effective radiation dose while maintaining image quality.

Materials and Methods

This study received approval from the Institutional Review Board (reference number: 45102721.8.0000.5083).

Assessment of CBCT radiation exposure

In this experimental study, an anthropomorphic Alderson RANDO Phantom (ART-200, RSD Phantoms, Long Beach, CA, USA) and 152 calibrated dosimeters (3 mm × 3 mm × 1 mm - titanium magnesium-doped lithium fluoride thermoluminescent dosimeters (TLDs); TLD 200; Harshaw, Solon, OH, USA) were utilized to evaluate the radiation dose

emitted by a CBCT Picasso Trio device (Vatech, Hwaseong, South Korea) employing 8 different protocols with varying milliamperage, kilovoltage peak, and number of projection images, as outlined in Table 1.

The selected phantom represents the average anatomical characteristics of an adult male (1.75 m tall and 73 kg) and is divided into 9 slices with a thickness of 2.5 cm. The phantom contains multiple 5-mm-diameter holes, allowing the placement of dosimeters to measure the radiation dose in different regions of the head and neck. The positioning of the phantom closely mimicked the conditions experienced by a patient during a CBCT scan (Fig. 1). Subsequently, for each of the 8 acquisition protocols, 19 TLDs were uniformly positioned in different regions of the phantom to represent various radiosensitive organs (Fig. 2 and Table 2).⁵⁻⁷ To account for potential variations in the X-ray energy produced during a single CBCT exposure, 5 repeated exposures were performed for each protocol. This approach considered the do-



Fig. 1. Alderson Rando anthropomorphic phantom (model ART-200, RSD Phantoms, Long Beach, CA, USA).

Table 1. Image acquisition protocols used with the Picasso Trio device (Vatech, Hwaseong, Korea) without metal artifact reduction

Protocol	Field of view (cm)	Voxel	Milliamperage (mA)	Kilovoltage peak (kVp)	Number of projection images
1	12 × 8.5	0.2	3	80	450
2	12 × 8.5	0.2	5	80	450
3	12 × 8.5	0.2	3	80	720
4	12 × 8.5	0.2	5	80	720
5	12 × 8.5	0.2	3	99	450
6	12 × 8.5	0.2	5	99	450
7	12 × 8.5	0.2	3	99	720
8	12 × 8.5	0.2	5	99	720



Fig. 2. Distribution of the 9 anatomical slices in the Alderson Rando phantom. Each level corresponds to the site of dosimeter insertion, as described in Table 2.

Table 2. Location of thermoluminescent dosimeters (TLDs) in the different sites and levels of the phantom

Organ	Site	Level
Bone marrow	Anterior calvarium	2
	Posterior calvarium	2
Cervical spine	Central branch (right)	6
	Central branch (left)	6
	Right ramus	6
	Left ramus	6
Mandible	Right body	7
	Left body	7
Brain	Middle brain	2
	Center of brain	3
Eyes	Right lens	4
	Left lens	4
Salivary glands	Right parotid gland	5
	Left parotid gland	5
	Right submandibular gland	7
	Left submandibular gland	7
	Right sublingual gland	7
	Left sublingual gland	7
Thyroid	Middle thyroid	9
Skin	Left nape	7
	Right cheek	5

simeters' sensitivity and aimed to obtain a reliable measurement of the radiation dose. The average of the 5 exposures was used to determine the radiation dose value. Background radiation measurements were obtained by fixing 3 TLDs to the external wall of the acquisition room. After exposure,

Table 3. Fraction of irradiated tissue (%) for calculating the absorbed dose

Organ	Irradiated fraction (%)
Bone marrow	16.5 (weighted in)
Mandible	1.3
Calvarium	11.8
Cervical spine	3.4
Thyroid	100
Skin	5
Bone surface	16.5 (weighted in)
Mandible	1.3
Calvarium	11.8
Cervical spine	3.4
Salivary glands	100 (weighted in)
Parotid	100
Submandibular	100
Sublingual	100
Brain	100
Remaining	
Lymph nodes	5
Muscle	5
Extrathoracic airways	100
Oral mucosa	100

the TLDs were analyzed using a Harshaw TLD Model 3500 reader (Thermo Scientific, Waltham, MA, USA).

The equivalent and effective doses for each organ were calculated using the following formula: $HT = WR \times \sum fi \times DTi$, where "WR" represents the radiation weighting factor (X-rays have a weighting factor of 1), "fi" denotes the fraction irradiated (Table 3), and "DTi" represents the average absorbed dose of tissue T in the corresponding slice. The effective dose was then determined using the formula: $E = WT \times HT$, where "E" is the product of the "WT" (the tissue weighting factor) and "HT" (the human-equivalent dose for the tissue). The tissue weighting factor indicates the relative contribution of each tissue or organ to the overall risk. The dose measurements were expressed in microsieverts (μSv).

Image quality evaluation

Three calibrated experts in oral radiology, with different levels of experience in CBCT (3, 10, and 15 years, respectively), examined the CBCT DICOM volumes obtained from the 8 protocols in the axial, coronal, and sagittal planes using CS 3D Imaging Software version 3.1.9 (Carestream Health, Rochester, NY, USA). The experts analyzed predetermined anatomical structures, assessed their confidence in identifying these structures, and documented their subjective im-

pression of the image quality, using the following classification: structure – 0) not identifiable, 1) partially identifiable, or 2) identifiable; quality – 1) excellent, 2) good, 3) acceptable, 4) poor, or 5) very poor; confidence – 1) not confident, 2) slightly confident, 3) confident, 4) very confident, or 5) extremely confident.

The following 12 anatomical structures were evaluated: the maxillary sinus, nasal cavity, incisive foramen, enamel, dentin, root canal, trabecular bone, lamina dura, periodontal ligament, alveolar crest, mental foramen, and mandibular canal. The examiners were blinded to the protocols and were allowed to adjust the brightness, contrast, and gray levels for better visualization of anatomical structures.

After a 15-day interval, 30% of the images were reassessed to analyze inter- and intra-observer reproducibility.

Statistical analysis

Statistical analysis was conducted using SPSS version 24.0 (IBM Corp., Armonk, NY, USA). The relationship between image quality and confidence rated by evaluators 1, 2, and 3 was assessed using the Fisher exact test. The agreement among raters 1, 2, and 3 was evaluated using the kappa test. Multiple linear regression analysis was performed to investigate whether the milliamperage, kilovoltage peak, and number of projection images could predict the effective dose. *P*-values < 0.05 were considered to indicate statistical significance.

Results

The effective dose values for each organ using different acquisition protocols are presented in Table 4. The calcu-

lation of the effective dose followed the recommendations of the International Commission on Radiological Protection (ICRP Publication 103, 2007).⁸ When comparing the 8 protocols tested in this study, the parameter that obtained the lowest effective radiation dose (224 μSv) was protocol 1 (3 mA; 80 kVp; 450 projection images), which used the lowest values of milliamperage, kilovoltage peak, and projection images. The protocol that obtained the highest effective radiation dose (909 μSv) was protocol 8 (5 mA; 99 kVp; 720 projection images), which used the maximum values of the acquisition parameters.

The experts faced no difficulty in identifying anatomical structures, even when the image quality was categorized as “very poor” (Table 5). An examination of the relationship between image quality and confidence, as perceived by evaluators 1, 2, and 3, revealed consistent values for all 12 analyzed structures (*P* < 0.05). However, discrepancies in the assessment of image quality were noted for the enamel (Expert 1 vs. Expert 2), trabecular bone (Expert 1 vs. Expert 2, Expert 2 vs. Expert 3), hard palate (Expert 1 vs. Expert 2), (Expert 2 vs. Expert 3), periodontal ligament (Expert 1 vs. Expert 2), (Expert 2 vs. Expert 3), and alveolar crest (Expert 1 vs. Expert 2), (Expert 2 vs. Expert 3) (Tables 6 and 7). The intra-observer agreement is presented in Table 8. These findings indicate no discernible effects on the experts’ confidence in the identification of anatomical structures.

Multiple linear regression was used to determine whether the milliamperage, kilovoltage peak, and projection images could predict the effective dose. The analysis resulted in a statistically significant model [F(3,4) = 13.862; *P* = 0.014, *R*² = 0.912]. The milliamperage (*b* = 0.504; *t* = 3.406; *P* = 0.027),

Table 4. Calculation of effective dose (μSv) following International Commission on Radiological Protection (ICRP, 2007) for different organs according to the protocols

Organ	Weighting factor	P1	P2	P3	P4	P5	P6	P7	P8
Bone marrow	0.12	20	31	32	45	34	52	53	79
Thyroid	0.04	18	25	24	39	23	40	40	71
Skin	0.01	2	3	3	4	3	5	5	8
Bone surface	0.01	6	9	10	14	8	12	13	19
Salivary glands	0.01	110	165	189	249	182	264	265	450
Brain	0.01	4	6	6	8	7	10	11	19
Remaining									
Lymph nodes	0.12	19	29	32	43	32	46	46	77
Muscle	0.12	19	29	32	43	32	46	46	77
Extrathoracic airways	0.12	376	579	642	862	636	925	928	1538
Oral mucosa	0.12	422	649	722	964	712	1027	1030	1732
Total		224	338	375	506	366	540	544	909

Table 5. Experts' proficiency in identifying predetermined anatomical structures and their subjective evaluations of image quality and confidence*

	Protocol	Identification expert 1	Identification expert 2	Identification expert 3	Quality expert 1	Quality expert 2	Quality expert 3	Confidence expert 1	Confidence expert 2	Confidence expert 3	Effective dose
Maxillary sinus	P1	3	3	3	4	5	5	4	5	5	224
	P2	3	3	3	4	5	5	4	5	5	338
	P3	3	3	3	4	5	5	4	5	5	375
	P4	3	3	3	4	5	5	5	5	5	506
	P5	3	3	3	4	5	5	5	5	5	366
	P6	3	3	3	4	5	5	5	5	5	540
	P7	3	3	3	4	5	5	4	5	5	544
	P8	3	3	3	4	5	5	4	5	5	909
Nasal cavity	P1	3	3	3	4	5	5	4	5	5	224
	P2	3	3	3	4	5	5	4	5	5	338
	P3	3	3	3	4	5	3	5	5	5	375
	P4	3	3	2	4	5	2	4	5	4	506
	P5	3	3	2	4	5	2	5	5	4	366
	P6	3	3	2	4	5	2	5	5	5	540
	P7	3	3	2	4	5	2	4	5	5	544
	P8	3	3	2	4	5	2	4	5	5	909
Incisive foramen	P1	3	3	3	4	4	5	4	5	5	224
	P2	3	3	3	4	4	5	4	5	5	338
	P3	3	3	3	4	4	5	4	5	5	375
	P4	3	3	3	4	4	5	5	5	5	506
	P5	3	3	3	4	4	5	4	5	5	366
	P6	3	3	3	4	4	5	5	5	5	540
	P7	3	3	3	4	4	5	4	5	5	544
	P8	3	3	3	4	5	5	4	5	5	909
Enamel	P1	3	3	3	4	4	5	4	5	5	224
	P2	3	3	3	4	4	5	4	5	5	338
	P3	3	3	3	4	5	5	4	5	5	375
	P4	3	3	3	4	4	5	4	5	5	506
	P5	3	3	3	4	4	5	4	5	5	366
	P6	3	3	3	4	4	5	5	4	5	540
	P7	3	3	3	4	4	5	5	5	5	544
	P8	3	3	3	4	4	5	4	5	5	909
Dentin	P1	3	3	3	4	4	5	4	5	5	224
	P2	3	3	3	4	4	5	4	5	5	338
	P3	3	3	3	4	5	5	4	5	5	375
	P4	3	3	3	4	3	4	4	4	5	506
	P5	3	3	3	4	4	5	4	5	5	366
	P6	3	3	3	4	4	5	5	4	5	540
	P7	3	3	3	4	4	5	5	5	5	544
	P8	3	3	3	4	4	5	5	5	5	909
Root canal	P1	3	3	3	4	3	5	4	5	5	224
	P2	3	3	3	4	4	5	5	5	5	338
	P3	3	3	3	4	5	5	4	5	5	375
	P4	3	3	3	4	5	5	4	5	5	506
	P5	3	3	3	4	5	5	5	5	5	366
	P6	3	3	3	4	4	5	5	5	5	540
	P7	3	3	3	4	4	5	5	5	5	544
	P8	3	3	3	4	4	5	4	5	5	909

Table 5. Continued

	Protocol	Identification expert 1	Identification expert 2	Identification expert 3	Quality expert 1	Quality expert 2	Quality expert 3	Confidence expert 1	Confidence expert 2	Confidence expert 3	Effective dose
Trabecular bone	P1	3	3	3	4	3	5	4	5	5	224
	P2	3	3	3	4	3	5	5	5	5	338
	P3	3	3	3	4	3	5	4	3	5	375
	P4	3	3	3	4	2	5	4	3	5	506
	P5	3	3	3	4	2	5	4	4	5	366
	P6	3	3	3	4	2	5	4	3	5	540
	P7	3	3	3	4	3	5	5	4	5	544
	P8	3	3	3	4	3	5	4	4	5	909
Periortal ligament/lamina dura	P1	3	1	2	3	1	3	3	3	4	224
	P2	3	2	2	4	2	3	4	3	4	338
	P3	3	2	1	4	2	2	4	3	4	375
	P4	3	1	1	3	1	3	4	3	4	506
	P5	3	1	1	4	1	2	4	3	4	366
	P6	2	1	1	2	1	2	3	3	4	540
	P7	2	1	2	3	2	2	3	3	4	544
	P8	2	2	2	3	2	2	3	3	4	909
Alveolar crest	P1	3	2	3	4	2	5	4	3	5	224
	P2	3	2	3	4	2	5	4	3	5	338
	P3	3	3	3	4	2	5	4	3	5	375
	P4	3	3	3	4	2	5	4	3	5	506
	P5	3	3	3	4	2	5	4	3	5	366
	P6	3	3	3	4	2	5	4	3	5	540
	P7	3	3	3	4	2	5	4	3	5	544
	P8	3	3	3	4	2	5	4	3	5	909
Mental foramen	P1	3	3	3	4	4	3	4	5	5	224
	P2	3	3	3	4	3	4	5	5	5	338
	P3	3	3	3	4	4	5	5	5	5	375
	P4	3	3	3	5	3	5	5	5	5	506
	P5	3	3	3	4	3	5	5	4	5	366
	P6	3	3	3	4	3	5	5	4	5	540
	P7	3	3	3	4	3	5	5	4	5	544
	P8	3	3	3	4	3	5	5	4	5	909
Mandibular canal	P1	3	3	3	4	3	5	5	5	5	224
	P2	3	3	3	4	4	5	5	5	5	338
	P3	3	3	3	4	4	5	5	5	5	375
	P4	3	3	3	5	4	5	5	5	5	506
	P5	3	3	3	4	3	5	5	4	5	366
	P6	3	3	3	4	3	5	5	4	5	540
	P7	3	3	3	4	3	5	5	4	5	544
	P8	3	3	3	4	3	5	5	4	5	909

Identification – 0: not identifiable, 1: partially identifiable, 2: identifiable; quality – 1: excellent, 2: good, 3: acceptable, 4: poor, 5: very poor; confidence – 1: not confident, 2: slightly confident, 3: confident, 4: very confident, 5: extremely confident

kilovoltage peak ($b=0.589$; $t=3.979$; $P=0.016$), and number of projection images ($b=0.557$; $t=3.762$; $P=0.020$) were predictors of the effective dose. The multiple linear regression analysis yielded the equation $y = -1,464.54 + 98$ (milliamperage) $+ 12.05$ (kilovoltage peak) $+ 0.802$ (projec-

tion images). All these analyses were supported by the correlation between the technical image acquisition parameters of each protocol and the effective dose in specific organs, as well as the total effective dose, as presented in Table 9.

Protocol 5, characterized by one of the lowest total effec-

Table 6. Kappa agreement analysis of evaluators 1, 2, and 3 regarding image quality ($P < 0.05$)

Image quality	Agreement between	Kappa (κ)
Maxillary sinus	Evaluator 1 - Evaluator 2	1.000
	Evaluator 1 - Evaluator 3	1.000
	Evaluator 2 - Evaluator 3	1.000
Nasal cavity	Evaluator 1 - Evaluator 2	1.000
	Evaluator 1 - Evaluator 3	0.000
	Evaluator 2 - Evaluator 3	0.000
Incisive foramen	Evaluator 1 - Evaluator 2	1.000
	Evaluator 1 - Evaluator 3	1.000
	Evaluator 2 - Evaluator 3	1.000
Enamel	Evaluator 1 - Evaluator 2	0.000
	Evaluator 1 - Evaluator 3	1.000
	Evaluator 2 - Evaluator 3	1.000
Dentin	Evaluator 1 - Evaluator 2	1.000
	Evaluator 1 - Evaluator 3	1.000
	Evaluator 2 - Evaluator 3	1.000
Root canal	Evaluator 1 - Evaluator 2	1.000
	Evaluator 1 - Evaluator 3	1.000
	Evaluator 2 - Evaluator 3	1.000
Trabecular bone	Evaluator 1 - Evaluator 2	0.000
	Evaluator 1 - Evaluator 3	1.000
	Evaluator 2 - Evaluator 3	0.000
Hard palate	Evaluator 1 - Evaluator 2	0.000
	Evaluator 1 - Evaluator 3	0.158
	Evaluator 2 - Evaluator 3	0.000
Periodontal ligament	Evaluator 1 - Evaluator 2	0.000
	Evaluator 1 - Evaluator 3	1.000
	Evaluator 2 - Evaluator 3	0.000
Alveolar crest	Evaluator 1 - Evaluator 2	0.000
	Evaluator 1 - Evaluator 3	1.000
	Evaluator 2 - Evaluator 3	0.000
Mental foramen	Evaluator 1 - Evaluator 2	1.000
	Evaluator 1 - Evaluator 3	1.000
	Evaluator 2 - Evaluator 3	1.000
Mandibular canal	Evaluator 1 - Evaluator 2	1.000
	Evaluator 1 - Evaluator 3	1.000
	Evaluator 2 - Evaluator 3	1.000

tive dose values (366 μ Sv) and diminished values in critical organs such as the bone marrow and thyroid, demonstrated a reduction ranging from -34.6% to -67.6% in sensitive organs compared to high-resolution protocols (protocols 6, 7, and 8). Notably, the adjustment of kilovoltage peak and the reduction of milliamperage (protocols 4 vs. 5) yielded diagnostically acceptable images, as evidenced by nearly a 48% reduction in the effective dose.

It is noteworthy that all 8 protocols yielded acceptable image quality (Fig. 3). Protocol 5 (3 mA; 99 kVp; 450 pro-

Table 7. Kappa agreement analysis of the evaluators' confidence in various structures ($P < 0.05$)

Structures	Agreement between	Kappa (κ)
Maxillary sinus	Evaluator 1 - Evaluator 2	1.000
	Evaluator 1 - Evaluator 3	1.000
	Evaluator 2 - Evaluator 3	1.000
Nasal cavity	Evaluator 1 - Evaluator 2	1.000
	Evaluator 1 - Evaluator 3	1.000
	Evaluator 2 - Evaluator 3	1.000
Incisive foramen	Evaluator 1 - Evaluator 2	1.000
	Evaluator 1 - Evaluator 3	1.000
	Evaluator 2 - Evaluator 3	1.000
Enamel	Evaluator 1 - Evaluator 2	1.000
	Evaluator 1 - Evaluator 3	1.000
	Evaluator 2 - Evaluator 3	1.000
Dentin	Evaluator 1 - Evaluator 2	1.000
	Evaluator 1 - Evaluator 3	1.000
	Evaluator 2 - Evaluator 3	1.000
Root canal	Evaluator 1 - Evaluator 2	1.000
	Evaluator 1 - Evaluator 3	1.000
	Evaluator 2 - Evaluator 3	1.000
Trabecular bone	Evaluator 1 - Evaluator 2	1.000
	Evaluator 1 - Evaluator 3	1.000
	Evaluator 2 - Evaluator 3	1.000
Hard palate	Evaluator 1 - Evaluator 2	1.000
	Evaluator 1 - Evaluator 3	1.000
	Evaluator 2 - Evaluator 3	1.000
Periodontal ligament	Evaluator 1 - Evaluator 2	1.000
	Evaluator 1 - Evaluator 3	1.000
	Evaluator 2 - Evaluator 3	1.000
Alveolar crest	Evaluator 1 - Evaluator 2	1.000
	Evaluator 1 - Evaluator 3	1.000
	Evaluator 2 - Evaluator 3	1.000
Mental foramen	Evaluator 1 - Evaluator 2	1.000
	Evaluator 1 - Evaluator 3	1.000
	Evaluator 2 - Evaluator 3	1.000
Mandibular canal	Evaluator 1 - Evaluator 2	1.000
	Evaluator 1 - Evaluator 3	1.000
	Evaluator 2 - Evaluator 3	1.000

Table 8. Intraobserver kappa agreement analysis regarding image quality and confidence in various structures

	Evaluator 1	Evaluator 2	Evaluator 3
Image quality	-0.452	0.485	0.592
Confidence	-0.658	0.732	-0.116

jection images) emerged as the optimized protocol for the evaluated structures. It exhibited commendable image qual-

Table 9. Relationship between milliamperage, kilovoltage peak, the number of projection images, and effective dose

Protocol	Field of view (cm)	Voxel size	Milliamperage (mA)	Kilovoltage peak (kVp)	Projection images (no.)	Bone marrow	Thyroid	Skin	Bone surface	Salivary glands	Brain	Lymph nodes	Muscle	Extrathoracic airways	Oral mucosa	Total effective dose (μ Sv)
1	12 × 8.5	0.2	3	80	450	20	18	2	6	110	4	19	19	376	422	224
2	12 × 8.5	0.2	5	80	450	31	25	3	9	165	6	29	29	579	649	338
3	12 × 8.5	0.2	3	80	720	32	24	3	10	189	6	32	32	642	722	375
4	12 × 8.5	0.2	5	80	720	45	39	4	14	249	8	43	43	862	964	506
5	12 × 8.5	0.2	3	99	450	34	23	3	8	182	7	32	32	636	712	366
6	12 × 8.5	0.2	5	99	450	52	40	5	12	264	10	46	46	925	1027	540
7	12 × 8.5	0.2	3	99	720	53	40	5	13	265	11	46	46	928	1030	544
8	12 × 8.5	0.2	5	99	720	79	71	8	19	450	19	77	77	1538	1732	909

ity assessment scores across all evaluators ($P < 0.05$) and relatively low effective dose values for radiation-sensitive organs, all while maintaining acquisition parameters at the lowest feasible levels.

Discussion

This investigation identified an optimized image acquisition protocol by using lower milliamperage values and fewer projection images, along with compensatory increases in kilovoltage peak. To achieve this, a CBCT device was employed that allows the operator to choose the parameters independently. While this might initially appear to limit the generalizability of the results, it proved indispensable for understanding the nuanced behavior of each parameter under investigation. These parameter adjustments made it possible to achieve good image quality while significantly reducing the effective radiation dose to the sensitive head and neck organs. When compared to similar protocols with higher milliamperage values (protocol 6) and higher number of projection images (protocol 7), the optimized protocol resulted in a 47% and 48% decrease in the effective dose, respectively. Importantly, the optimized protocol maintained the same level of concordance and confidence among evaluators as high-radiation dose protocols ($P < 0.05$), suggesting that the acquired image quality is acceptable.

The potential molecular effects of CBCT radiation are uncertain, and no specific threshold has been established. Therefore, optimizing the radiation dose in CBCT exams is crucial for improving patient protection against the harmful effects of ionizing radiation. These effects are associated with potential changes in DNA and an increased risk of oncogenesis.⁹ The approach proposed in this study focuses on optimizing the effective radiation dose, which is the most appropriate metric for measuring the overall risk of stochastic effects from radiation exposure. This approach also considers the impact on image quality. Although diagnostic efficacy for a particular task was not specifically evaluated, this study assessed radiologists' confidence in identifying anatomical structures using different CBCT protocols through a subjective evaluation, revealing high confidence levels. This suggests that the image quality was acceptable for diagnostic purposes, even in lower-dose protocols. Another important strength of the present study was the adoption of an effective dose prediction model, which was obtained through multiple linear regression analysis. The analysis resulted in a statistically significant model, with milliamperage identified as the most significant predictor of the effective dose.

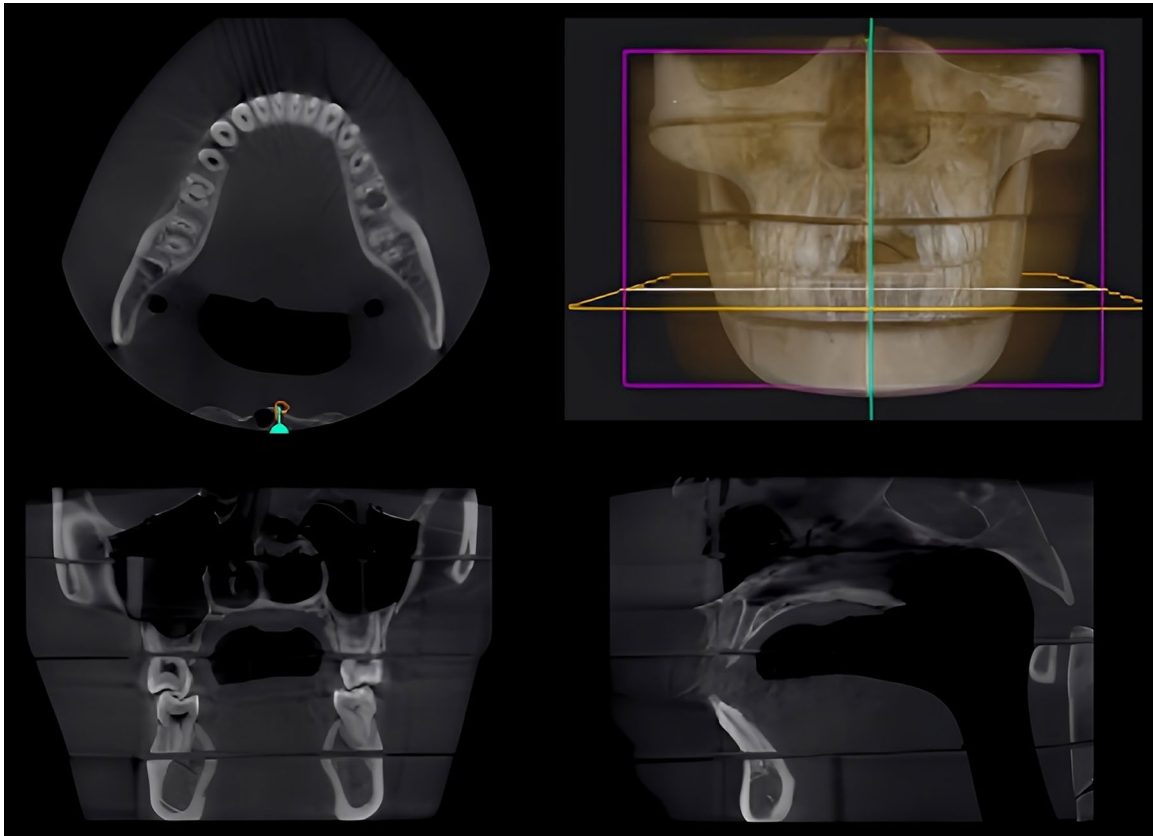


Fig. 3. Axial, coronal, and sagittal cone-beam computed tomography reconstructions show the image quality achieved with protocol 5 (3 mA; 99 kVp; 450 projection images), which was identified as the optimized protocol.

Various factors contribute to changes in the effective dose emitted by different CBCT devices, highlighting the need for further research to evaluate the efficacy of different dose reduction methods and establish correlations with image quality.⁴ This study analyzed the influence of distinctive CBCT acquisition protocols on reducing the effective radiation dose while maintaining image quality, using TLD and an anthropomorphic phantom. This method provides accurate radiation dose measurements by considering the X-ray attenuation characteristics of the human body. However, the lack of standards for the location and number of TLDs in the phantom limits the reproducibility of the results.¹⁰ Different technical parameters have been demonstrated to influence the effective dose in various CBCT devices.¹¹⁻¹⁴ The 3 main exposure parameters tested in this study were milliamperage, kilovoltage peak, and the number of projection images, which showed a substantial impact on the effective dose.

The increase in milliamperage is directly proportional to the increase in effective dose, and related to the decrease in image noise, which is important for image quality.¹⁰ Nevertheless, the beam penetration and contrast are influenced by

kilovoltage peak. The increase in kilovoltage peak also has an impact on the effective dose, but this effect is not linear, with its increase impacting the radiation dose less than milliamperage.¹⁰ In the present study, the lower values of milliamperage with compensatory higher values of kilovoltage peak significantly reduced the effective dose levels and maintained image quality.

The influence of CBCT exposure parameters on image quality was previously assessed by Al-Okshi et al.¹⁵ They found that CBCT radiation exposure was affected not only by the FOV, but also by acquisition parameters such as milliamperage and kilovoltage peak. These parameters had an impact on both the quantity and quality of the incident radiation, which aligns with the observations in the present investigation and emphasizes the effect on radiation dose. The dimensions of FOV are known to influence the effective dose from CBCT devices, suggesting that the FOV should be kept as small as possible in cases where high-quality images are necessary.¹⁶ In the present study, the FOV was kept at the same size in all protocols and was not tested for variation.

Despite the promising results found here, it is essential

to interpret them with caution. In dosimetry, several factors must be considered regarding effective doses, such as the type of phantom used, the number and placement of dosimeters, the equipment type, and its parameters (milliamperage, kilovoltage peak, FOV, exposure time, and voxel size). Different combinations of these parameters can result in varying doses.^{6,17,18} Several studies evaluating CBCT scans have shown a wide range of effective doses, and even when comparing the same equipment model, the results may be inconsistent.^{6,19-23}

Another crucial consideration when comparing radiation dose levels is the weighting factor used to calculate the dose for each tissue or organ. In 2007, the ICRP included the oral mucosa, salivary glands, and extrathoracic airways as radiosensitive tissues and proposed specific weighting factors in its 103rd publication, replacing the recommendations from 1990.⁸ These changes in tissue weighting factors and the inclusion of salivary glands in the ICRP 2007 recommendations led to an increase in effective dose.²² The present study followed the 2007 recommendations. Therefore, for a proper interpretation of the results, the dose levels obtained here should be compared with studies using the same guidelines and similar CBCT devices.^{22,24}

Regarding studies investigating the Picasso Trio device using the ICRP 2007 recommendations, Pauwels et al. (2012)²⁵ evaluated the effective dose using 2 protocols (low-dose and high-dose). They maintained the acquisition parameters of FOV (12 × 7 cm) and kilovoltage peak (85 kVp) in both protocols, changing only the milliamperage value. They found lower effective dose values than those found in the present study, which can be explained by the smaller FOV used. In another investigation that also evaluated radiation dose in the Picasso Trio equipment, Hofmann et al. (2014)²⁶ calculated the absorbed dose of radiosensitive organs. They used a FOV of 12 × 7 cm, 5.5 mA, 85 kVp, and a voxel size of 0.2 mm. The absorbed dose values they found were lower for the brain, eyes, and bone surface than was observed in all protocols in the present study. However, in the thyroid, the dose values found in this study were lower in protocols 1, 2, and 3, suggesting that lower kilovoltage peak values might help reduce the absorbed radiation in this specific region. However, comparing different dosimetric studies could be questionable, even when using the same CBCT device.

In principle, the parameters adopted in this study to optimize the acquisition protocol, with a reduction in milliamperage and a compensatory increase in kilovoltage peak, could be applied to optimize CBCT in other scans. As mentioned before, other technical parameters can influence the

image quality and dose, and these parameters can vary greatly among the various CBCT equipment available on the market. Therefore, it may not always be possible to alter the milliamperage and kilovoltage peak in specific CBCT systems, underscoring the need for device-specific research to improve pre-programmed protocols established by CBCT equipment developers. Additionally, oral and maxillofacial radiologists should have a thorough understanding of CBCT's technical parameters to optimize acquisition protocols for various patients and different diagnostic tasks in dental clinics. Consequently, the radiation dose must be optimized in each device to ensure that the acquisition protocol provides an image that is diagnostically acceptable for a specific patient and indication-oriented, as reflected in the ALADAIP principle (“as low as diagnostically acceptable being indication-oriented and patient-specific”).²⁷

The results of the present study showed that optimizing milliamperage, kilovoltage peak, and the number of projection images can reduce the effective dose without compromising radiologists' confidence in the acquired images. However, caution is necessary when interpreting the results due to various factors that influence effective dose calculations, including the phantom type, dosimeter placement, equipment parameters, and dose calculation guidelines. Consistency in tissue weighting factors is crucial for accurate dose comparisons. Further research is needed to explore parameter optimization in different diagnostic tasks and devices, ensuring diagnostically acceptable images with minimal radiation exposure.

Conflicts of Interest: None

References

1. European Commission. Radiation protection No 172. Cone beam CT for dental and maxillofacial radiology. Evidence based guidelines [Internet]. Luxembourg: Publications Office of the European Union; 2012 [cited 2023 Nov 20]. Available from: https://sedentext.eu/files/radiation_protection_172_1.pdf.
2. Jaju PP, Jaju SP. Cone-beam computed tomography: time to move from ALARA to ALADA. *Imaging Sci Dent* 2015; 45: 263-5.
3. De Grauwe A, Ayaz I, Shujaat S, Dimitrov S, Gbadegbegnon L, Vande Vannet B, et al. CBCT in orthodontics: a systematic review on justification of CBCT in a paediatric population prior orthodontic treatment. *Eur J Orthod* 2019; 41: 381-9.
4. da Silva Moura W, Chiqueto K, Pithon GM, Neves LS, Castro R, Henriques JFC. Factors influencing the effective dose associated with CBCT: a systematic review. *Clin Oral Investig* 2019; 23: 1319-30.
5. Ludlow JB, Davies-Ludlow LE, Brooks SL. Dosimetry of two extraoral direct digital imaging devices: NewTom cone beam

- CT and Orthophos Plus DS panoramic unit. *Dentomaxillofac Radiol* 2003; 32: 229-34.
6. Ludlow JB, Davies-Ludlow LE, Brooks SL, Howerton WB. Dosimetry of 3 CBCT devices for oral and maxillofacial radiology: CB Mercuray, NewTom 3G and i-CAT. *Dentomaxillofac Radiol* 2006; 35: 219-26.
 7. Martins LAC, Brasil DM, Forner LA, Viccari C, Haiter-Neto F, Freitas DQ, et al. Does dose optimisation in digital panoramic radiography affect diagnostic performance? *Clin Oral Investig* 2021; 25: 637-43.
 8. Clero E, Vaillant L, Zhang W, Hamada N, Preston DL, Laurier D, et al. ICRP publication 152: radiation detriment calculation methodology. *Ann ICRP* 2022; 51: 1-103.
 9. Belmans N, Gilles L, Vermeesen R, Virag P, Hedesiu M, Salmon B, et al. Quantification of DNA double strand breaks and oxidation response in children and adults undergoing dental CBCT scan. *Sci Rep* 2020; 10: 2113.
 10. McGuigan MB, Duncan HF, Horner K. An analysis of effective dose optimization and its impact on image quality and diagnostic efficacy relating to dental cone beam computed tomography (CBCT). *Swiss Dent J* 2018; 128: 297-316.
 11. Kadesjö N, Benchimol D, Falahat B, Näsström K, Shi XQ. Evaluation of the effective dose of cone beam CT and multislice CT for temporomandibular joint examinations at optimized exposure levels. *Dentomaxillofac Radiol* 2015; 44: 20150041.
 12. Pauwels R, Zhang G, Theodorakou C, Walker A, Bosmans H, Jacobs R, et al. Effective radiation dose and eye lens dose in dental cone beam CT: effect of field of view and angle of rotation. *Br J Radiol* 2014; 87: 20130654.
 13. Palomo JM, Rao PS, Hans MG. Influence of CBCT exposure conditions on radiation dose. *Oral Surg Oral Med Oral Pathol Oral Radiol Endod* 2008; 105: 773-82.
 14. Jadu F, Yaffe MJ, Lam EW. A comparative study of the effective radiation doses from cone beam computed tomography and plain radiography for sialography. *Dentomaxillofac Radiol* 2010; 39: 257-63.
 15. Al-Okshi A, Theodorakou C, Lindh C. Dose optimization for assessment of periodontal structures in cone beam CT examinations. *Dentomaxillofac Radiol* 2017; 46: 20160311.
 16. Ihlis RL, Kadesjö N, Tsilingaridis G, Benchimol D, Shi XQ. Image quality assessment of low-dose protocols in cone beam computed tomography of the anterior maxilla. *Oral Surg Oral Med Oral Pathol Oral Radiol* 2022; 133: 483-91.
 17. Ludlow JB, Ivanovic M. Comparative dosimetry of dental CBCT devices and 64-slice CT for oral and maxillofacial radiology. *Oral Surg Oral Med Oral Pathol Oral Radiol Endod* 2008; 106: 106-14.
 18. Helmrot E, Thilander-Klang A. Methods for monitoring patient dose in dental radiology. *Radiat Prot Dosimetry* 2010; 139: 303-5.
 19. Chinem LA, Vilella Bde S, Maurício CL, Canevaro LV, Deluiz LF, Vilella Ode V. Digital orthodontic radiographic set versus cone-beam computed tomography: an evaluation of the effective dose. *Dental Press J Orthod* 2016; 21: 66-72.
 20. Roberts JA, Drage NA, Davies J, Thomas DW. Effective dose from cone beam CT examinations in dentistry. *Br J Radiol* 2009; 82: 35-40.
 21. Ludlow JB, Walker C. Assessment of phantom dosimetry and image quality of i-CAT FLX cone-beam computed tomography. *Am J Orthod Dentofacial Orthop* 2013; 144: 802-17.
 22. Grünheid T, Kolbeck-Schieck JR, Pliska BT, Ahmad M, Larson BE. Dosimetry of a cone-beam computed tomography machine compared with a digital x-ray machine in orthodontic imaging. *Am J Orthod Dentofacial Orthop* 2012; 141: 436-43.
 23. Ludlow JB. A manufacturer's role in reducing the dose of cone beam computed tomography examinations: effect of beam filtration. *Dentomaxillofac Radiol* 2011; 40: 115-22.
 24. Loubele M, Bogaerts R, Van Dijck E, Pauwels R, Vanheusden S, Suetens P, et al. Comparison between effective radiation dose of CBCT and MSCT scanners for dentomaxillofacial applications. *Eur J Radiol* 2009; 71: 461-8.
 25. Pauwels R, Beinsberger J, Collaert B, Theodorakou C, Rogers J, Walker A, et al. Effective dose range for dental cone beam computed tomography scanners. *Eur J Radiol* 2012; 81: 267-71.
 26. Hofmann E, Schmid M, Sedlmair M, Banckwitz R, Hirschfelder U, Lell M. Comparative study of image quality and radiation dose of cone beam and low-dose multislice computed tomography - an in-vitro investigation. *Clin Oral Investig* 2014; 18: 301-11.
 27. Oenning AC, Jacobs R, Salmon B, DIMITRA Research Group (<http://www.dimitra.be>). ALADAIP, beyond ALARA and towards personalized optimization for paediatric cone-beam CT. *Int J Paediatr Dent* 2021; 31: 676-8.